Aquatic Toxicology 142–143 (2013) 347–354

Contents lists available at ScienceDirect

Aquatic Toxicology

journal homepage: www.elsevier.com/locate/aquatox

Studies on the toxicity of an aqueous suspension of C_{60} nanoparticles using a bacterium (*gen. Bacillus*) and an aquatic plant (*Lemna gibba*) as *in vitro* model systems

Sandra M.A. Santos[a], Augusto M. Dinis[b,c], David M.F. Rodrigues[d], Francisco Peixoto[e], Romeu A. Videira[d,1], Amália S. Jurado[a,c,*,1]

[a] CNC – Centre for Neuroscience and Cell Biology, University of Coimbra, Coimbra, Portugal
[b] Laboratory of Electron Microscopy and Palynology and Centre for Functional Ecology, University of Coimbra, Coimbra, Portugal
[c] Department of Life Sciences, University of Coimbra, Coimbra, Portugal
[d] CECAV, Department of Chemistry, University of Trás-os-Montes e Alto Douro, Vila Real, Portugal
[e] CITAB, Department of Chemistry, University of Trás-os-Montes e Alto Douro, Vila Real, Portugal

ARTICLE INFO

Article history:
Received 12 May 2013
Received in revised form 4 August 2013
Accepted 1 September 2013

Keywords:
Fullerene
Bacterial growth
Bacterial respiration
Chlorophylls
Chloroplast oxygen production

ABSTRACT

The increasing use of C_{60} nanoparticles and the diversity of their applications in industry and medicine has led to their production in a large scale. C_{60} release into wastewaters and the possible accumulation in the environment has raised concerns about their ecotoxicological impact. In the present study, an aqueous suspension of C_{60} nanoparticles was prepared and its potential toxicity studied in laboratory, using a bacterium (*Bacillus stearothermophilus*) and an aquatic plant (*Lemna gibba*) as model systems. C_{60} nanoparticles inhibited the growth of *L. gibb*a, in contrast to that of the bacterium. Consistently, the ultrastructure and respiratory activity of bacterial cells were not affected by C_{60}, but the contents of chlorophylls a and b and chloroplast oxygen production decreased considerably in *L. gibba*. Altogether, our results suggest that C_{60} aqueous dispersions must be viewed as an environmental pollutant, potentially endangering the equilibrium of aquatic ecosystems.

1. Introduction

Fullerenes are molecular cages containing from 28 to more than 100 carbon atoms, which correspond to a nano-sized group of carbon allotropes with large surface area and high reactivity (Kroto et al., 1985). The distinctive physicochemical properties of fullerenes have allowed the development of products with unprecedent characteristics and applications in many fields of human activity, thus having tremendous economic impacts (Bakry et al., 2007; Bosi et al., 2003; Yadav and Kumar, 2008). C_{60}, the most representative among fullerenes (Kroto et al., 1985), and its water-soluble derivatives are produced in a large scale due to their multiple applications in material science and biomedicine (Bakry et al., 2007; Benn et al., 2011; Bosi et al., 2003; Markovic and Trajkovic, 2008; Partha and Conyers, 2009). The increased likelihood of C_{60} direct release into wastewaters and its accumulation in the environment (Benn et al., 2011; Gottschalk et al., 2009) has raised concern about its health and ecological effects (Owen and Handy, 2007). Toxicological studies have shown that C_{60} nanoparticles are able to induce toxicity linked with oxidative stress in several cell lines in culture and whole animal systems (Oberdörster, 2004; Sayes et al., 2005; Usenko et al., 2008). C_{60} molecules absorb in the UV and visible range of light spectrum and, in the presence of molecular oxygen, can generate ROS, particularly singlet oxygen and superoxide anion (Brunet et al., 2009; Guldi and Asmus, 1999; Hotze et al., 2008; Pickering and Wiesner, 2005). Therefore, when C_{60} is released into the environment and activated by sunlight, inducing the production of ROS, it may endanger live organisms due to the reaction of ROS with proteins, nucleic acids and the double bonds of membrane phospholipid hydrocarbon chains, which will lead to downstream detrimental effects, such as protein and DNA adduction, lipid peroxidation, membrane rupture and, eventually, cell death (Halliwell and Gutteridge, 2007). However, the molecular mechanisms underlying the toxicity of nano-C_{60} water suspensions remain a controversial issue (Spohn et al., 2009). On the other hand, the toxicity of C_{60} nanoparticle dispersions toward live organisms has shown high variability, depending on the methods used to prepare C_{60} suspensions (see Shinohara et al., 2008 and references therein).

* Corresponding author at: CNC – Centre for Neuroscience and Cell Biology, Largo Marquês de Pombal, University of Coimbra, 3004-517 Coimbra, Portugal. Tel.: +351 239 853600; fax: +351 239 853409.
E-mail address: asjurado@bioq.uc.pt (A.S. Jurado).
[1] Both authors share senior authorship.

0166-445X/$ – see front matter © 2013 Elsevier B.V. All rights reserved.
http://dx.doi.org/10.1016/j.aquatox.2013.09.001

The present work aims to further clarify the toxicological activity of C_{60} fullerene in aqueous dispersions devoid of residual organic solvents and to determine the influence of light on the susceptibility of biological systems to C_{60} nanoparticles. With this purpose, toxicological assays were performed using a microorganism-model (*Bacillus stearothermophilus*) and an aquatic photosynthetic organism (*Lemna gibba*), both of which have shown to be good tools to study the toxicity of a variety of pollutants (Perreault et al., 2010; Pereira et al., 2009; Cayuela et al., 2007; Monteiro et al., 2005; Lewis, 1995). Considering these two aerobic organisms, we hypothesize that the light-dependent metabolism of *L. gibba* would make it more susceptible to the toxic effects of C_{60} fullerene. In this context, the following strategy was established: (a) to prepare a stable aqueous suspension of C_{60} devoid of tetrahydrofuran; (b) to test its safety or toxicity taking as physiological endpoints the bacterial growth and respiration and *L. gibba* growth, chloroplast oxygen production and chlorophyll content.

The results obtained in the present study, concerning the effects of C_{60} on the two biological models at the level of growth and metabolic processes, namely respiratory activity in *B. stearothermophilus* and photosynthesis in *L. gibba*, suggest that the environmental impact exerted by C_{60} nanoparticles might be closely related to their photoactivation and that the organisms mostly affected in ecosystems might be those which depend on light as energy source.

2. Materials and methods

2.1. Chemicals

C_{60} and the other chemicals used in the present work were obtained from Sigma Chemical Company (St. Louis, MO, USA) and were of highest commercially available quality.

2.2. Preparation of an aqueous suspension of C_{60} nanoparticles

C_{60} aqueous suspensions were prepared transferring fullerene nanoparticles from toluene solution into the aqueous phase using ultrasonic treatment, as described elsewhere (Andrievsky et al., 2002) with some modifications. Briefly, 4 mg of solid C_{60} were added to 2 mL of toluene and stirred for several minutes to yield a purple solution. This solution was then added to 100 mL of deionized ultrapure water and stirred vigorously to promote formation of an emulsion of toluene in water. The emulsion was sonicated (50 W, 40 KHz) for 24 h in water bath to remove toluene by evaporation and to promote the transfer of the C_{60} nanoparticles into the aqueous phase. The mixture was filtered under reduced pressure through a cellulose nitrate filter with a pore size of 450 nm to remove the solid material and agglomerates of particles with an average size above 450 nm. The filtered colloidal suspension was transferred to a round bottom flask and approximately half the solvent evaporated in a rotatory evaporator, at 50 °C, to concentrate the sample and remove any traces of toluene. Residual toluene amounts in C_{60} aqueous suspensions were evaluated by GC/MS after headspace solid-phase microextraction (SPME) between the fullerene and carboxen-polydimethylsiloxane fibers, using 30 min of equilibrium at 40 °C (Lee et al., 2007).

2.3. Determination of the concentration of C_{60} nanoparticles

The concentration of C_{60} nanoparticles in the aqueous suspension was determined by UV-visible spectrophotometry. The spectrum in the range of 200–700 nm was recorded with 1 nm resolution, using a Lambda 45 UV/visible spectrophotometer (Perkin Elmer). The C_{60} molar absorption coefficient (ε) at 343 nm of 68,000 dm^3 / mol/cm was used for calculating C_{60} concentration in the aqueous suspension (Andrievsky et al., 2002).

2.4. Determination of the size and Zeta potential of C_{60} nanoparticles

The size distribution and Zeta potential of C_{60} nanoparticles in the aqueous suspension were determined with a Zeta Plus analyzer (Brookhaven). The average diameter of C_{60} aqueous suspension was determined by dynamic light scattering (DLS) at 25 °C, using a helium-neon laser wavelength of 658 nm and a detector angle of 90°. The Zeta potential measurements were performed at 25 °C and pH 7 measuring electrophoretic mobility using phase analysis light scattering, as described by Brant et al. (2005).

2.5. Bacterial strain and growth conditions

The strain of *B. stearothermophilus* and the conditions for its maintenance and growth have been described previously (Jurado et al., 1987). *B. stearothermophilus* was grown at 65 °C in 250 mL Erlenmeyer flasks containing 50 mL of L-Broth medium, in a New Brunswick water bath shaker, at 100 rpm. Aliquots of a C_{60} aqueous suspension (from a few μL to 5.0 mL) were added to 50 mL of growth medium before inoculation in order to obtain concentrations ranging from 2 to 15 mg/L, and water was added to make a final volume of 55 mL to all the flasks. Flasks containing 50 mL of growth medium and 5 mL of water, without addition of C_{60} nanoparticles, were prepared for control cultures. A bacterial suspension in the logarithmic growth phase was used to inoculate fresh media with or without C_{60} nanoparticles, in order to obtain an initial optical density at 610 nm of 0.03, which corresponds to a cell density of $1 \times 10^6 \pm 0.05 \times 10^6$ viable cells (bacterial colony-forming unit counts) per milliliter of growth medium. The bacterial growth was measured by turbidimetry at 610 nm in a Jenway 6405 spectrophotometer. Aliquots of the growth medium not inoculated with cells, containing 0–15 mg/L of C_{60} and exposed to the conditions (65 °C and 100 rpm) at which bacteria were grown, were used as blanks, their optical density at 610 nm being measured at each time-point. However, the optical density of blanks, at this wavelength, was always very low at our experimental conditions.

2.6. Bacterial cell ultrastructure

B. stearothermophilus cultures grown in L-Broth in the absence (control) or in the presence of C_{60} nanoparticles (15 mg/L) were harvested in the logarithmic growth phase and twenty milliliters of culture suspension was mixed with two milliliters of glutaraldehyde 25%. Then, cell suspensions were centrifuged at 10,000 g for 5 min at 4 °C in a refrigerated centrifuge (Sorvall, Thermo Scientific) and the supernatant was neglected. The cells were further resuspended in glutaraldehyde 2.5% in 0.1 M cacodylate buffer, pH 7.0. After 4 h of incubation, the cells were washed twice with 50 mL of cacodylate buffer supplemented with 10 mL $CaCl_2$ (pH 6.4) and fixed at room temperature, for 2 h, in 1% buffered osmium tetroxide (OsO_4) (Silva and Macedo, 1983). Following fixation, the samples were dehydrated with a graded ethanol series and embedded in Spurr. Ultrathin sections were cut with an ultramicrotome LKB Ultrotome NOVA equipped with a diamond knife, and conventionally stained with uranyl acetate and lead citrate. Observations were made with a JEOL JEM-100SX at 80 kV.

2.7. Measurement of oxygen consumption rate in bacterial protoplasts

Oxygen consumption was measured in protoplasts of *B. stearothermophilus* obtained from cells of cultures grown as

mentioned above, under control conditions (without C_{60} nanoparticles added) and harvested in the middle of the exponential growth phase. The preparation of protoplast suspension by cell incubation with lysozyme was previously described (Donato et al., 1997). Protoplast protein content was determined by the Biuret method and oxygen consumption was monitored polarographically with a Clark oxygen electrode (Estabrook, 1967) in a thermostated water-jacketed closed chamber containing 1 mL of reaction medium (40 mM Hepes–Tris, 10 mM MgCl2, pH 7.5) with magnetic stirring, at 40 °C. Protoplasts (0.1 mg protein) were incubated 5 min in the reaction medium containing C_{60} nanoparticles in the concentration range of 10–200 μg/mg protein or without C_{60} added (control). The effect of C_{60} on protoplast oxygen consumption was evaluated using NADH (5 mM) as respiratory substrate.

2.8. Cultures of L. gibba

L. gibba plants were collected from an artificial pond in the Portuguese Vila Real de Trás-os-Montes e Alto Douro University campus and placed in an aquarium containing 5 L of half-strength Hutner's medium (Brain and Solomon, 2007). The aquarium was placed in a culture growth chamber (Conviron mod. E7/2) at 20 ± 2 °C and under 50 μmol/m^2/s photosynthetically active radiation (PAR) provided by a set of cool white fluorescent Osram Sylvania tube lamps. The light/dark cycle was adjusted to 16 h/8 h and the cultures were subcultured twice a week (Juhel et al., 2011). Plants were maintained in culture for eight weeks prior to be used in toxicological assays.

2.9. Exposure of L. gibba to C_{60} nanoparticles and growth evaluation

The effects of increasing concentrations of C_{60} nanoparticles on *L. gibba* cultures at the exponential phase, after seven days of growth, were assessed considering the frond number and the fresh weight, according to standard guideline 221 (OECD, 2002). Thirty *L. gibba* fronds were gently placed in crystallizing cups containing 15 mL of fresh growth medium and aliquots of C_{60} nanoparticles (from a few μL to 1.1 mL) were added from a concentrated aqueous suspension, in order to obtain concentrations ranging from 1 to 10 mg C_{60}/L. Plants were incubated at 20 ± 2 °C under a photosynthetically active radiation (50 μmol/m^2/s), for 7 days in a culture growth chamber (Conviron mod. E7/2). The relative growth rate (RGR) was calculated according to the following equation: $RGR = (\ln x_2 - \ln x_1)/(t_2 - t_1)$, where x_1 and x_2 are the frond number at time t_1 (0 days) and t_2 (7 days), respectively (Kufel et al., 2012).

2.10. Chlorophyll extraction and quantification

Chlorophyll content of *L. gibba* exposed during 7 days to different concentrations of C_{60} nanoparticles were also evaluated. Plants of each crystallizing cups were homogenized in 5 mL of 80% (v/v) acetone solution with a Potter homogenizer. The homogenates were maintained overnight in a freezer and then filtered. The optical density of chlorophyll extracts was measured at 663 and 646 nm in a spectrophotometer (Bio-Varian 100) and the concentrations of chlorophyll a (Chl a), chlorophyll b (Chl b) and total chlorophyll were calculated by the following equations: Chl a (μg/mL) = $12.21A_{663} - 2.81A_{646}$ and Chl b (μg/mL) = $20.13A_{646} - 5.03A_{663}$; total chlorophyll = Chl a + Chl b (Lichtenthater and Wellburn, 1983). All values were normalized with respect to plant fresh weight.

2.11. Chloroplast isolation

L. gibba chloroplasts were isolated as described by Babu et al. (2001) with minor modifications. Approximately 35 g of *L. gibba* plants in isolation buffer (345 mM sorbitol, 5 mM $MgCl_2$, 1 g polyclar, 4 mM tricine-NaOH, pH 8) were homogenized with a blender homogeneizer (sterilmixer 12, poliBrand), for 4 pulses of 5 s, at 4 °C. The homogenate was filtered through eight layers of cheesecloth (Calbiochem, La Jolla, CA, USA) and the filtrate was centrifuged at 1500 g (Sigma 2 K) for 5 min at 4 °C. The supernatant was rejected and the pellet resuspended in 25 mL of isolation buffer and centrifuged at 1500 g for 5 min at 4 °C. The pellet corresponding to the isolated chloroplasts was resuspended in 1 mL of isolation buffer and stored at 4 °C in the dark. 30 μL of butylated hydroxytoluene (BHT) was added to the isolated chloroplasts to avoid peroxidation of membranes lipids. The final concentration of chloroplasts was evaluated in terms of total chlorophyll (Chl a + Chl b) content, measuring the absorbance at 663 and 646 nm in a spectrophotometer (Bio-Varian 100), as mentioned above.

2.12. Measurement of oxygen production rate in L. gibba chloroplasts

The photosynthetic activity of isolated chloroplasts was evaluated by measuring the oxygen production using a Clark-type oxygen electrode (Hansatech, Norfolk, UK) coupled to a computer, as previously described by Babu et al. (2001) with some modifications. A volume of the chloroplast fraction corresponding to 75 μg of total chlorophylls (Chl a + Chl b) was placed in a thermostated water-jacketed glass chamber with magnetic stirring at 20 °C, containing 2 mL of standard reaction medium (345 mM sorbitol, 2 mM $MgCl_2$, 2 mM tricine-NaOH pH 8.4) supplemented with 1 μM sodium azide and 1.25 μM methyl viologen (MV^{2+}). After a dark pre-incubation for 2 min, the reaction was initiated by switching on the light source (1000 μmol/m^2/s photosynthetically active radiation) and oxygen production was followed continuously. After 2 min, light was turned off, to confirm that oxygen changes were strictly light dependent, and switched on again to add a specific inhibitor of photosynthesis (3-(3,4-dichlorophenyl)-1,1-dimethylurea; DCMU 5.0 μM), in order to guarantee that oxygen changes were due to chloroplast photosynthesis activity. Aliquots from a concentrated aqueous suspension of C_{60} nanoparticles were added to 2 mL standard reaction medium supplemented with chloroplasts, to obtain fullerene concentrations ranging 1–10 mg/L. The preparations were incubated for 2 min in the dark, before starting the photosynthetic activity by switching on the light source. Data acquisition and treatment (chloroplast oxygen production rates) were carried out using an appropriate software (Oxylab ver 1.15 Hansatech, Norfolk, UK).

2.13. Statistical analysis

All the values were expressed as mean ± standard deviation of at least three independent experiments. The values were statistically compared through one-way ANOVA with the Student–Newman–Keuls as post-test. Statistical significance was set at $p < 0.05$.

3. Results

3.1. Characterization of C_{60} aqueous suspensions

The size distribution of C_{60} nanoparticles in aqueous suspensions, evaluated by dynamic light scattering analysis, is shown in Fig. 1. In water suspensions, C_{60} nanoparticles exhibited a size ranging from 29 to 38 nm, with a predominant population with an

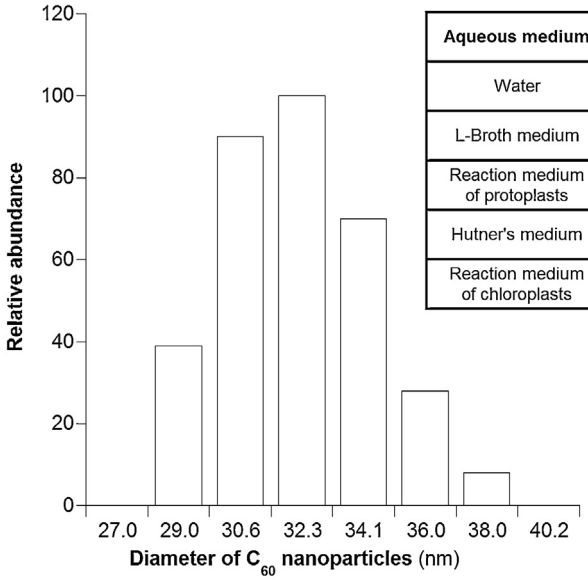

Aqueous medium	Size (nm)	Zeta potencial (mV)
Water	32.8 ± 4.9	-24.6 ± 3.8
L-Broth medium	34.9 ± 3.5	-21.8 ± 1.9
Reaction medium of protoplasts	43.4 ± 5.6	-20.8 ± 4.9
Hutner's medium	78.5 ± 8.2	-21.7 ± 1.3
Reaction medium of chloroplasts	28.0 ± 3.1	-20.8 ± 4.1

Fig. 1. Number-weighted size distribution of C_{60} nanoparticles in aqueous suspensions determined by Dynamic Light Scattering. A table with size and Zeta potential acquired by the nanoparticles in different aqueous media is represented as an inset.

average diameter of 32.3 nm. Additionally, C_{60} nanoparticles displayed a negative surface charge (Zeta potential of -24.6 ± 3.8 mV), which was not affected by the composition of the growth or reaction media, as shown in the inset of Fig. 1. However, regarding the size distribution of C_{60} nanoparticles, the Hutner's medium (used for Lemna growth) promoted larger clusters (78.5 ± 8.2 nm), reflecting the role of the high ionic strength in the agglomeration process of nanoparticles. Noteworthy, the size values of C_{60} nanoparticles indicated in the insert of Fig. 1 were reproduced in aqueous suspensions at the maximal fullerene concentration used in growth assays (10 and 15 mg/L), under stirring, over the time of the respective experiments.

3.2. Effects of C_{60} on the growth of *B. stearothermophilus*

Fig. 2 shows the effects of increasing concentrations of C_{60} on the growth of *B. stearothermophilus* in L-Broth medium at 65 °C (optimal temperature). The addition of C_{60} in the concentration range of 2–15 mg/L did not exert appreciable effects on bacterial growth (Fig. 2A), although a significant decrease (about 6%) in the maximal cell density reached at the stationary phase was noticed in the presence of C_{60} at the concentration of 15 mg/L (Fig. 2A and B). The lag phase length (Fig. 2A) and the specific growth rate (Fig. 2A and B) were not affected by C_{60} nanoparticles, at the concentrations assayed. Noteworthy, at these C_{60} concentrations, no agglomeration was noticed till the end of the experiment.

3.3. Effect of C_{60} on the ultrastructure of *B. stearothermophilus*

The morphology of *B. stearothermophilus* cells (rod-shaped), analyzed by TEM (Fig. 3), showed no alterations when harvested from cultures grown without (control) or with 15 mg/L of C_{60} nanoparticles at the logarithmic growth phase (60 min of growth). In both conditions, the cytoplasm appeared finely granular with evenly distributed ribosomes, and the plasma membrane densely stained, with the typical asymmetric geometry.

3.4. Effect of C_{60} on the oxygen consumption of *B. stearothermophilus* protoplasts

The effects of C_{60} on the oxygen consumption rate of bacterial protoplasts are shown in Fig. 4. The advantage of using protoplasts (cells devoid of cell wall) instead of whole cells in this study resides in the easier accessibility of the compounds under study (C_{60} nanoparticles) and the respiratory substrates (NADH) to the bacterial respiratory system localized in the cytoplasmic membrane. On the other hand, toxicological studies using protoplasts of this bacterium have provided data comparable to those obtained with rat liver mitochondria (Donato et al., 1997; Pereira et al., 2009).

Protoplasts, prepared from cells of *B. stearothermophilus* grown in the basal medium and incubated in the presence of C_{60} nanoparticles in the concentration range of 10–200 μg/mg of protein showed a respiratory activity supported by NADH very similar to that of protoplasts to which C_{60} nanoparticles were not added (control).

3.5. Effect of C_{60} on *L. gibba* growth rate and chlorophyll content

L. gibba growth in the absence and in the presence of increasing C_{60} nanoparticles concentrations (1–10 mg/L) was assessed after a period of seven days to evaluate the effects of fullerene nanoparticles on vegetative proliferation. As shown in Fig. 5A, *L. gibba* growth rate, assessed by counting the frond number, decreased progressively with increasing concentrations of C_{60} nanoparticles. The impact of aquatic plant exposure to fullerene on chlorophyll contents was also evaluated in order to correlate the inhibition of plant vegetative proliferation with the functional state of chloroplasts, which is highly dependent on chlorophyll content and thylakoid membrane organization. Fig. 5B shows that C_{60} nanoparticles significantly decreased both chlorophyll a (Chl a) and chlorophyll b (Chl b) contents in *L. gibba*, reaching a maximal effect at a concentration of 2 mg/L.

3.6. Effects of C_{60} on oxygen production rate of *L. gibba* chloroplasts

The functional impact of C_{60} nanoparticles on photosynthetic activity of *L. gibba* was investigated by following their effect on

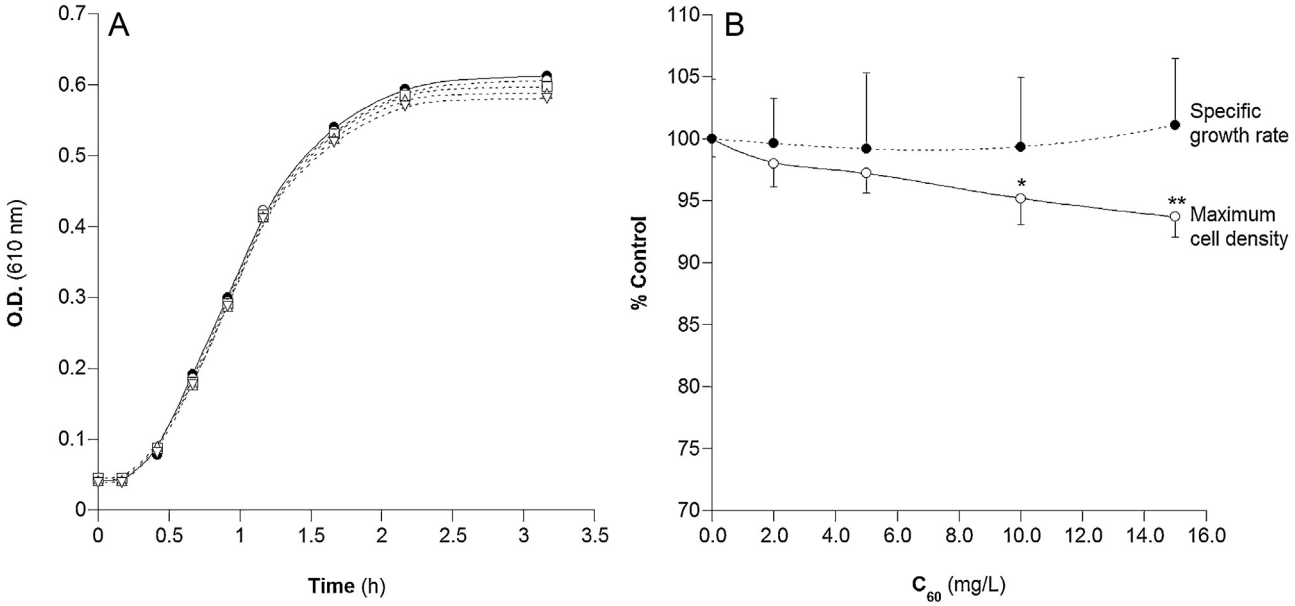

Fig. 2. Effects of C_{60} nanoparticles on the growth of *B. stearothermophilus*, at 65 °C (optimal growth temperature). Cells were grown in L-Broth medium in the absence (●), or in the presence of 2 mg/L (○), 5 mg/L (□), 10 mg/L (△) and 15 mg/L (▽) of C_{60} nanoparticles. (A) Growth curves obtained by measuring the optical density (O.D.) of bacterial cultures in liquid medium, at 610 nm. The results shown are typical of three independent experiments. (B) Specific growth rates and maximal cell densities reached in the stationary phase of cultures of *B. stearothermophilus* grown in media containing different concentrations of C_{60}. Data are expressed as percentage of those obtained with a control culture (grown in the absence of C_{60} nanoparticles). All results are presented as mean ± standard deviation of at least three independent experiments. Data comparisons were performed between cultures treated with C_{60} nanoparticles and the control culture, using one-way ANOVA with the Student–Newman–Keuls as post-test ($^{*}p < 0.05$; $^{**}p < 0.01$).

oxygen production rate of isolated chloroplasts. In these assays, triggered by light, molecules of H_2O acted as electron donors to the photosynthetic electron transport chain and MV^{2+} was used as the final electron acceptor, which delivered stoichiometrically the electrons to O_2. Therefore, the chloroplast photosynthetic activity was assessed recording the oxygen decrease in the reaction chamber (Babu et al., 2001). A progressive decrease in oxygen production rate was noticed with increasing C_{60} concentrations up to 15 mg/L (Fig. 6), denoting an inhibition of chloroplast activity.

4. Discussion

The paucity of toxicological data on carbon nanoparticles makes it difficult to forecast the risks arising from exposure to those nanomaterials, whose widespread application may lead to an extensive environmental contamination. Several evidences of the negative impact of fullerenes on soil microorganisms (Johansen et al., 2008) and aquatic organisms, such as Daphnia and fish (Lovern and Klaper, 2006; Zhu et al., 2006), can be found in literature. However, the absence of adverse effects has also been reported for soil microbial communities (Tong et al., 2007).

Since C_{60} nanoparticles are very hydrophobic, their incorporation within the hydrophobic core of lipid bilayer may be anticipated. In fact, computer simulation studies (Chang and Violi, 2006) have proposed this location for C_{60} nanoparticles and predicted a perturbation of membrane lipid packing with eventual destabilization of the bilayer. However, studies conducted by Aquino et al. (2010) in *Escherichia coli* did not support C_{60}-induced disruption of the cell membrane, although inhibition of bacterial growth and reduction of cell viability had been observed in the

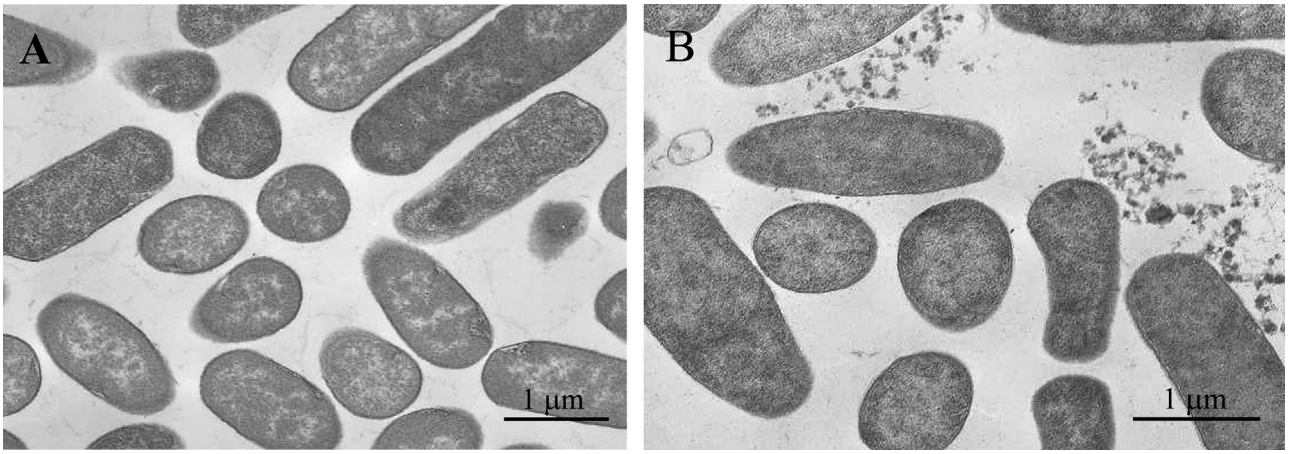

Fig. 3. Transmission electron micrographs of *B. stearothermophilus* cells from cultures grown without (control) (A) or with 15 mg/L of C_{60} (B), at the exponential phase of growth (after 60 min of growth). Typical populations of bacteria, with a densely stained plasma membrane, were observed in both treated and non-treated cultures, indicating that C_{60} nanoparticles, denoted in the micrograph as disperse aggregates, exerted no apparent adverse effects on bacterial cells.

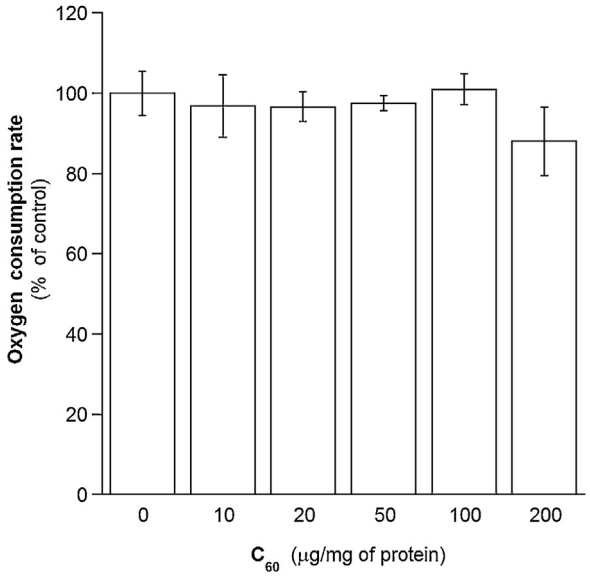

Fig. 4. Effects of C_{60} nanoparticles on the oxygen consumption rate of *B. stearothermophilus* protoplasts using NADH as substrate (5 mM). The oxygen consumption rate of protoplasts in the absence of C_{60} nanoparticles (control) was 233.8 ± 12.8 nmol O_2/min/mg protein. All results are means ± standard deviation from three independent experiments.

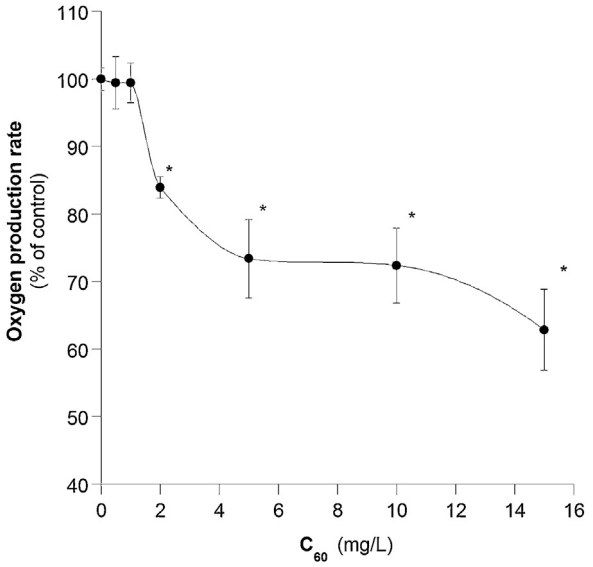

Fig. 6. Effects of C_{60} nanoparticles on the oxygen production rate of chloroplasts. Chloroplasts were isolated from *L. gibba*, and in the absence of C_{60} nanoparticles (control) the oxygen production rate was 77.3 ± 1.3 μmol O_2/mg of Chl ($a + b$)/h. All the results represent the mean ± standard deviation of three independent experiments and comparisons relative to the control were performed using one-way ANOVA with the Student-Newman-Keuls as post-test ($^*p < 0.05$).

presence of those nanoparticles. On the other hand, assays *in vitro* showed that a C_{60} nanoparticle suspension induced lipid peroxidation in the brain tissue of the common carp *Cyprinus carpio* under artificial light, but not in the dark condition (Shinohara et al., 2008). Therefore, in a toxicological context, the light seems to be an essential factor to be taken into account in studies aiming at understanding or predicting the biological effects of fullerenes. In fact, the photoactivation of C_{60} with UV/visible light, leading to its transition to a long-lived triplet excited state (Prat et al., 1999), fosters the formation of highly reactive singlet oxygen ($^1O_2$), as a consequence of the transfer of energy to molecular oxygen (Hirsch and Brettreich, 2005). The interactions of this and other ROS with biological targets have been evoked to explain the adverse effects of those nanoparticles mediated by oxidative stress. Thus, the pro-oxidant properties of C_{60} aqueous suspensions would make them a new type of dangerous chemical pollutant endangering a variety of organisms (Ferreira et al., 2012; Oberdörster, 2004). However, some controversy exists as to whether water-soluble nano-C_{60} is the primary material responsible for those pro-oxidant effects or if residual organic solvents (namely THF), used in some methods for preparation of C_{60} aqueous suspensions, are the actual inducers of the oxidative stress reported for C_{60} suspensions (Spohn et al., 2009). In fact, THF-nC_{60} (an aqueous C_{60} preparation obtained by using THF as solvent in a first step) has shown to be more toxic in bacteria, daphnia and fish than a nanoC_{60} suspension prepared without the presence of organic solvents (Fortner et al., 2005; Henry et al., 2007; Lovern and Klaper, 2006; Zhu et al., 2006). Therefore, in the present study, special attention has been paid to the preparation of the aqueous suspension of C_{60}, in which we rejected the use

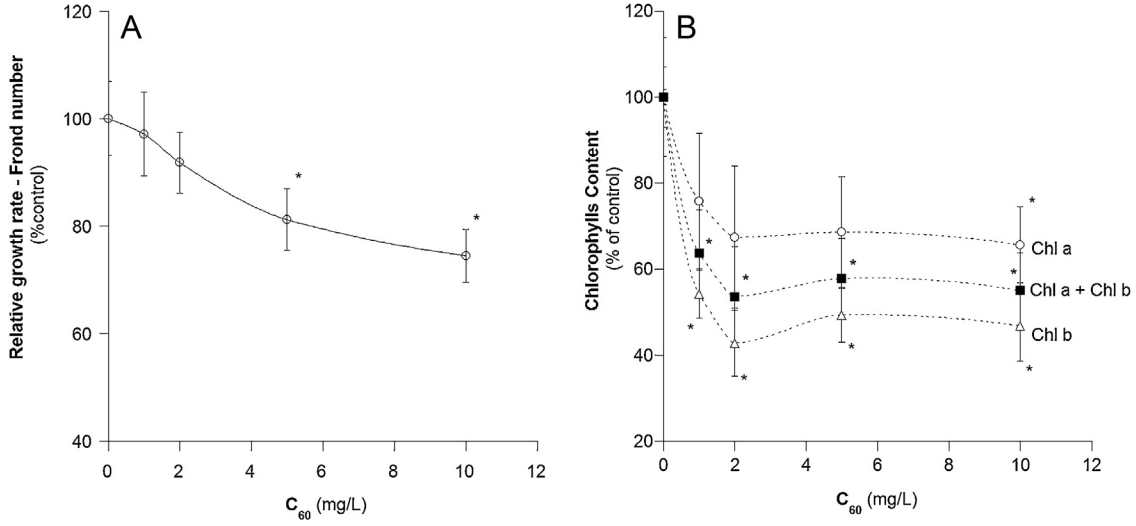

Fig. 5. Relative growth rate (A) and relative chlorophyll content (B) of *L. gibba* exposed for 7 days to increasing concentrations of C_{60} nanoparticles. The relative growth rate (RGR) was calculated as described in Material and Methods. Data are expressed as percentage of control (*L. gibba* grown in the absence of C_{60} nanoparticles). All results represent the mean ± standard deviation of three independent experiments and comparisons relative to the control were performed using one-way ANOVA with the Student–Newman–Keuls as post-test ($^*p < 0.05$).

of tetrahydrofuran (THF). Additionally, toluene was not detected by GC/MS after headspace SPME, indicating that the concentration of this solvent in our C_{60} aqueous suspensions was lower than 0.1 ng/mL (low detection limit obtained with toluene standard solutions).

In order to evaluate the environmental impact of water-soluble C_{60}, a bacterium (*B. stearothermophilus*) and an aquatic plant (*L. gibba*) were selected as model systems of typical members (a prokaryotic and an eukaryotic) of the lowest ecosystem trophic levels, which play a key role in nutrient cycling, thus underpinning ecosystem activity. *B. stearothermophilus* is a thermophilic Gram-positive eubacterium, which has shown to be sensitive to a wide range of pollutants assayed in our laboratory (Donato et al., 1997; Monteiro et al., 2005; Pereira et al., 2009). It has the advantage of being an easily handled microorganism, exhibiting a high specific growth rate in liquid cultures at high temperatures, which exclude eventual contaminations by other microorganisms. Moreover, this bacterium has shown high sensitivity to membrane-active compounds (Donato et al., 2000), among which hydrophobic C_{60} nanoparticles might be included, as previously suggested (Chang and Violi, 2006). Thus, studies in our laboratory have shown that alterations of membrane physical properties induced by lipophilic molecules result in inhibition of growth and impairment of the respiratory activity of *B. stearothermophilus* (Donato et al., 1997; Monteiro et al., 2005; Pereira et al., 2009). *L. gibba* is a sensitive aquatic plant often used in ecotoxicological studies due to their small size, simple structure, ease of handling and culture, high rate of growth and high sensitivity to a great variety of pollutants (Cayuela et al., 2007; Perreault et al., 2010). The evaluation of the inhibition of *Lemna* sp. growth in the presence of environmental pollutants has been considered a standard toxicity test by the United States Environmental Protection Agency (EPA, 1996). Growth inhibition in these organisms (Cayuela et al., 2007; Donato et al., 1997; Lewis, 1995; Monteiro et al., 2005; Pereira et al., 2009) as well as perturbations of vital functions, such as respiratory activity (Donato et al., 1997; Monteiro et al., 2005; Pereira et al., 2009) and photosynthesis (Babu et al., 2001; Huang et al., 1997; Perreault et al., 2010) have been revealed as good indicators of cytotoxicity. In the present work, limited effects were exerted by C_{60} nanoparticles on *B. stearothermophilus* growth at concentrations up to 15 mg/L. This discrepancy relative to other studies on microorganisms, such as that of Aquino et al. (2010) in *E. coli*, should be assigned to different C_{60} aqueous suspensions. In fact, those authors used THF in the C_{60} preparation method and we did not.

The morphology of *B. stearothermophilus* cells was also preserved at the maximal concentration of C_{60} nanoparticles assayed, as observed by electron microscopy (Fig. 3). Micrographs clearly show a very uniform population of rod-shaped cells, similar to those of the control culture. Although some fullerene agglomerates can be seen outside the cells in the fixed material, probably as a consequence of the centrifugation performed for cell sample preparation for TEM, no agglomeration was noticed in the Erlenmeyer flasks over the time of bacterial growth experiments, discarding the hypothesis that the absence of C_{60} effects was due to C_{60} precipitation.

As expected, C_{60} nanoparticles did not affect the NADH-supported respiratory activity of protoplasts, at concentrations up to 200 μg/mg of protein. However, *L. gibba* showed a decrease in growth by 25% after 7 days of exposure to the maximal C_{60} nanoparticles concentration assayed (10 mg/L), which seemed to be mechanistically related to the inhibition of photosynthesis, as assessed by measuring the oxygen production. Chloroplasts play crucial functions in plants, providing them with nutrients and energy for growth. These organelles contain specific pigments (such as chlorophylls and carotenoids) and an electron transfer chain for performing photosynthesis (Berg et al., 2002). The chlorophyll decay in plants exposed to fullerene constituted a significant physiological alteration, which was noticeable earlier than *L. gibba* growth perturbations. These data suggest that *in vivo* fullerene toxicity detected by growth inhibition could result from the impairment of chloroplast functionality, which might, in turn, have been a consequence of a direct action of C_{60} nanoparticles at the level of photosystem II (Hill reactions) or of perturbations in electron transfer between photosynthetic electron transport chain complexes. On the other hand, the more pronounced decrease of Chl b relative to Chl a in the presence of C_{60} (Fig. 5) should have led to an anomalous Chl a/Chl b ratio, which might result in damage in structural organization of light-harvesting complex (Dewez et al., 2003). The contents of Chl a and Chl b in *L. gibba* chloroplasts showed a maximal decrease (30 and 60%, respectively) in the presence of 2 mg/L of C_{60}. At this low concentration, the oxygen production by PSII was reduced in 15%, but a higher decrease (until 35%) occurred with C_{60} concentrations up to 15 mg/L. The apparent discrepancy between C_{60} concentrations that induced maximal decrease of chlorophyll content (*in vivo* studies) and maximal reduction of oxygen production (*in vitro* studies) suggests that, at concentrations above 2 mg/L, the progressive decrease of oxygen production rather than reflecting a direct impairing of the photosynthetic system might result from a concomitant oxidative process associated with ROS generation, putatively contributing to the dysfunction of photosystem II. This would result in additional inhibition of vegetative proliferation, consistent with the fact that C_{60} nanoparticles decreased oxygen production and inhibited growth of *L. gibba* in the same concentration range. However, due to the sorption ability of C_{60} nanoparticles, toward organic as well as inorganic molecules, C_{60}-induced growth inhibition of *L. gibba* could also reflect the decrease of micronutrients availability, as has been previously proposed to explain first-growing bacteria inhibition detected in soil microbial communities after C_{60} incorporation (Johansen et al., 2008).

Altogether, our results show that C_{60} nanoparticles at concentrations up to 10 mg/L exert severe toxic effects on *L. gibba*, but slight or null effects on *B. stearothermophilus* metabolism and growth. Taking into account that the organisms used in this study are models of representative elements of ecosystems putatively affected by residual waters containing fullerene nanoparticles, and that those organisms play an important role in nutrient cycling in nature, the fate of C_{60} nanoparticles in the environment arises as an important issue to deserve further investigation.

5. Conclusion

The results presented here suggest that *L. gibba* is more susceptible to the effects of C_{60} nanoparticles than *Bacillus stearothermophillus*. C_{60} nanoparticles affected the photosynthetic activity of *L. gibba* and inhibited its growth. Considering that *L. gibba* is a primary producer in aquatic food chains, the contamination of natural environment with C_{60} nanoparticles may have serious implications in the equilibrium of aquatic ecosystems.

Acknowledgements

This work was supported by the grants Pest-C/SAU/LA0001/2011 and PTDC/QUI-BIQ/103001/2008, funded by Portuguese Foundation for Science and Technology and COMPETE and FEDER. SMAS is the recipient of a fellowship from the Portuguese Foundation for Science and Technology (SFRH/BD/35285/2007).

References

Andrievsky, G.V., Klochkov, V.K., Bordyuh, A.B., Dovbeshko, G.I., 2002. Comparative analysis of two aqueous-colloidal solutions of C_{60} fullerene with help of FTIR reflectance and UV–Vis spectroscopy. Chem. Phys. Lett. 364, 8–17.

Aquino, A., Chan, J., Giolma, K., Loh, M., 2010. The effect of a fullerene water suspension on the growth, cell viability, and membrane integrity of *Escherichia coli* B23. J. Exp. Microbiol. Immunol. 14, 13–20.

Babu, T.S., Marder, J.B., Tripuranthakam, S., Dixon, D.G., Greenberg, B.M., 2001. Synergistic effects of a photooxidized polycyclic aromatic hydrocarbon and copper on photosynthesis and plant growth: evidence that in vivo formation of reactive oxygen species is a mechanism of copper toxicity. Environ. Toxicol. Chem. 20, 1351–1358.

Bakry, R., Vallant, R.M., Najam-ul-Haq, M., Rainer, M., Szabo, Z., Huck, C.W., Bonn, G.K., 2007. Medicinal applications of fullerenes. Int. J. Nanomedicine 2 (4), 639–649.

Benn, T.M., Westerhoff, P., Herckes, P., 2011. Detection of fullerenes (C_{60} and C_{70}) in commercial cosmetics. Environ. Pollut. 159, 1334–1342.

Berg, J.M., Tymoczko, J.L., Stryer, L., 2002. Biochemistry, 5th edition. W.H. Freeman, New York.

Bosi, S., Da Ros, T., Spalluto, G., Prato, M., 2003. Fullerene derivatives: an attractive tool for biological applications. Eur. J. Med. Chem. 38, 913–923.

Brain, R.A., Solomon, K.R., 2007. A protocol for conducting 7-day daily renewal tests with *Lemna gibba*. Nat. Protoc. 2, 979–987.

Brant, J., Lecoanet, H., Wiesner, M.R., 2005. Aggregation and deposition characteristics of fullerene nanoparticles in aqueous systems. J. Nanopart. Res. 7, 545–553.

Brunet, L., Lyon, D.Y., Hotze, E.M., Alvarez, P.J.J., Wiesner, M.R., 2009. Comparative photoactivity and antibacterial properties of C_{60} fullerenes and titanium dioxide nanoparticles. Environ. Sci. Technol. 43, 4355–4360.

Cayuela, M.L., Millner, P., Slovin, J., Roig, A., 2007. Duckweed (*Lemna gibba*) growth inhibition bioassay for evaluating the toxicity of olive mill wastes before and during composting. Chemosphere 68, 1985–1991.

Chang, R., Violi, A., 2006. Insights into the effect of combustion-generated carbon nanoparticles on biological membranes: a computer simulation study. J. Phys. Chem. B 110, 5073–5083.

Dewez, D., Dautremepuits, C., Jeandet, P., Vernet, G., Popovic, R., 2003. Effects of methanol on photosynthetic processes and growth of *Lemna gibba*. Photochem. Photobiol. 78, 420–424.

Donato, M.M., Jurado, A.S., Antunes-Madeira, M.C., Madeira, V.M., 1997. Comparative study of the toxic actions of 2,2-bis(p-chlorophenyl)-1,1,1-trichloroethane and 2,2-bis(p-chlorophenyl)-1,1-dichloroethylene on the growth and respiratory activity of a microorganism used as a model. Appl. Environ. Microbiol. 63, 4948–4951.

Donato, M.M., Jurado, A.S., Antunes-Madeira, M.C., Madeira, V.M., 2000. Membrane lipid composition of *Bacillus stearothermophilus* as affected by lipophilic environmental pollutants: an approach to membrane toxicity assessment. Arch. Environ. Contam. Toxicol. 39, 145–153.

EPA, 1996. Ecological Effects Test Guidelines OPPTS 850.4400. Aquatic Plant Toxicity Test using *Lemna* spp., Tiers I and II, EPA 712-C-96-156.

Estabrook, R.W., 1967. Mitochondrial respiratory control and the polarographic measurements of ADP/O ratios. Meth. Enzymol. 10, 41–47.

Ferreira, J.L.R., Barros, D.M., Geracitano, L.A., Fillmann, G., Fossa, C.E., de Almeida, E.A., de Castro Prado, M., Neves, B.R.A., Pinheiro, M.V.B., Monserrat, J.M., 2012. In vitro exposure to fullerene C_{60} influences redox state and lipid peroxidation in brain and gills from *Cyprinus carpio* (Cyprinidae). Environ. Toxicol. Chem. 31, 961–967.

Fortner, J.D., Lyon, D.Y., Sayes, C.M., Boyd, A.M., Falkner, J.C., Hotze, E.M., Alemany, L.B., Tao, Y.J., Guo, W., Ausman, K.D., Colvin, V.L., Hughes, J.B., 2005. C_{60} in water: nanocrystal formation and microbial response. Environ. Sci. Technol. 39, 4307–4316.

Gottschalk, F., Sonderer, T., Scholz, R.W., Nowack, B., 2009. Modeled environmental concentrations of engineered nanomaterials (TiO2, ZnO, Ag, CNT, fullerenes) for different regions. Environ. Sci. Technol. 43, 9216–9222.

Guldi, D.M., Asmus, K.-D., 1999. Activity of water-soluble fullerenes towards OH-radicals and molecular oxygen. Radiat. Phys. Chem. 56, 449–456.

Halliwell, B., Gutteridge, J.M.C., 2007. Free Radicals in Biology and Medicine, 4th edition. Oxford University Press Inc, New York.

Henry, T.B., Menn, F.M., Fleming, J.T., Wilgus, J., Compton, R.N., Sayler, G.S., 2007. Attributing effects of aqueous C_{60} nano-aggregates to tetrahydrofuran decomposition products in larval zebrafish by assessment of gene expression. Environ. Health Perspect. 115 (7), 1059–1065.

Hirsch, A., Brettreich, M., 2005. Fullerenes: Chemistry and Reactions. Wiley-VCH, Weinheim.

Hotze, E.M., Labille, J., Alvarez, P., Wiesner, M.R., 2008. Mechanisms of photochemistry and reactive oxygen production by fullerene suspensions in water. Environ. Sci. Technol. 42, 4175–4180.

Huang, X.-D., McConkey, B.J., Babu, T.S., Greenberg, B.M., 1997. Mechanisms of photoinduced toxicity of photomodified anthracene to plants: inhibition of photosynthesis in the aquatic higher plant *Lemna gibba* (duckweed). Environ. Toxicol. Chem. 16, 1707–1715.

Johansen, A., Pedersen, A.L., Jensen, K.A., Karlson, U., Hansen, B.M., Scott-Fordsmand, J.J., Winding, A., 2008. Effects of C_{60} fullerene nanoparticles on soil bacteria and protozoans. Environ. Toxicol. Chem. 27, 1895–1903.

Juhel, G., Batisse, E., Hugues, Q., Daly, D., van Pelt, F.N.A.M., O'Halloran, J., Jansen, M.A.K., 2011. Alumina nanoparticles enhance growth of *Lemna minor*. Aquat. Toxicol. 105, 328–336.

Jurado, A.S., Santana, A.C., Costa, M.S., Madeira, V.M.C., 1987. Influence of divalent cations on the growth and morphology of *Bacillus stearothermophilus*. J. Gen. Microbiol. 133, 507–513.

Kufel, L., Strzalek, M., Wysokińska, U., Biardzka, E., Oknińska, S., Rys, K., 2012. Growth rate of duckweeds (*Lemnaceae*) in relation to the internal and ambient nutrient concentrations – testing the droop and monod models. Pol. J. Ecol. 60 (2), 241–249.

Kroto, H.W., Heath, J.R., O'Brien, S.C., Curl, R.F., Smalley, R.E., 1985. C_{60}: buckminsterfullerene. Nature 318, 14.

Lee, M.-R., Chang, C.-M., Dou, J., 2007. Determination of benzene, toluene, ethylbenzene, xylenes in water at sub-ng l-1 levels by solid-phase microextraction coupled to cryo-trap gas chromatography-mass spectrometry. Chemosphere 69, 1381–1387.

Lewis, M.A., 1995. Use of freshwater plants for phytotoxicity testing: a review. Environ. Pollut. 87, 319–336.

Lichtenthater, H.K., Wellburn, A.R., 1983. Determinations of total carotenoids and chlorophylls a and b of leaf extracts in different solvents. Biochem. Soc. Trans. 11, 591–592.

Lovern, S.B., Klaper, R., 2006. *Daphnia magna* mortality when exposed to titanium dioxide and fullerene (C_{60}) nanoparticles. Environ. Toxicol. Chem. 25, 1132–1137.

Markovic, Z., Trajkovic, V., 2008. Biomedical potential of the reactive oxygen species generation and quenching by fullerenes (C_{60}). Biomaterials 29, 3561–3573.

Monteiro, J.P., Jurado, A.S., Moreno, A.J.M., Madeira, V.M.C., 2005. Toxicity of methoprene as assessed by the use of a model microorganism. Toxicol. In Vitro 19, 951–956.

Oberdörster, E., 2004. Manufactured nanomaterials (fullerenes, C_{60}) induce oxidative stress in the brain of juvenile largemouth bass. Environ. Health Perspect. 112, 10.

OECD, 2002. Guidelines for the Testing of Chemicals. Environment Directorate, Organisation for Economic Cooperation and Development, Paris, France.

Owen, R., Handy, M.H., 2007. Viewpoint: formulating the problems for environmental risk assessment of nanomaterials. Environ. Sci. Technol. 41, 5582–5588.

Partha, R., Conyers, J.L., 2009. Biomedical applications of functionalized fullerene-based nanomaterials. Int. J. Nanomedicine 4, 261–275.

Pereira, S.P., Fernandes, M.A.S., Martins, J.D., Santos, M.S., Moreno, A.J.M., Vicente, J.A.F., Videira, R.A., Jurado, A.S., 2009. Toxicity assessment of the herbicide metolachlor comparative effects on bacterial and mitochondrial model systems. Toxicol. In Vitro 23, 1585–1590.

Perreault, F., Oukarroum, A., Pirastru, L., Sirois, L., Gerson Matias, W., Popovic, R., 2010. Evaluation of copper oxide nanoparticles toxicity using chlorophyll a fluorescence imaging in *Lemna gibba*. J. Bot. 2010, 9.

Pickering, K.D., Wiesner, M.R., 2005. Fullerol-sensitized production of reactive oxygen species in aqueous solution. Environ. Sci. Technol. 39, 1359–1365.

Prat, F., Stackow, R., Bernstein, R., Qian, W., Rubin, Y., Foote, C.S., 1999. Triplet-state properties and singlet oxygen generation in a homologous series of functionalized fullerene derivatives. J. Phys. Chem. A 103, 7230–7235.

Sayes, C.M., Gobin, A.M., Ausman, K.D., Mendez, J., West, J.L., Colvin, V.L., 2005. Nano-C_{60} cytotoxicity is due to lipid peroxidation. Biomaterials 26, 7587–7595.

Shinohara, N., Matsumoto, T., Gamo, M., Miyauchi, A., Endo, S., Yonezawa, Y., Nakanishi, J., 2008. Is lipid peroxidation induced by the aqueous suspension of fullerene C_{60} nanoparticles in the brains of *Cyprinus carpio*? Environ. Sci. Technol. 43, 948–953.

Silva, M.T., Macedo, P., 1983. A comparative ultrastructural study of the membranes of *Mycobacterium leprae* and of cultivable Mycobacterium. Biol. Cell 47, 383–386.

Spohn, P., Hirsch, C., Hasler, F., Bruinink, A., Krug, H.F., Wick, P., 2009. C_{60} fullerene: a powerful antioxidant or a damaging agent? The importance of an in-depth material characterization prior to toxicity assays. Environ. Pollut. 157, 1134–1139.

Tong, Z., Bischoff, M., Nies, L., Applegate, B., Turco, R.F., 2007. Impact of fullerene (C_{60}) on a soil microbial community. Environ. Sci. Technol. 41, 2985–2991.

Usenko, C.Y., Harper, S.L., Tanguay, R.L., 2008. Fullerene C_{60} exposure elicits an oxidative stress response in embryonic zebrafish. Toxicol. Appl. Pharmacol. 229 (1), 44–55.

Yadav, B.C., Kumar, R., 2008. Structure, properties and applications of fullerenes. Int. J. Nanotechnol. Appl. 2, 15–24.

Zhu, S., Oberdörster, E., Haasch, M.L., 2006. Toxicity of an engineered nanoparticle (fullerene, C_{60}) in two aquatic species, *Daphnia* and *Fathead minnow*. Mar. Environ. Res. 62 (Supplement 1), S5–S9.